Symmetry Adapted way for the efficient Trotter decomposition

Bo Yang[1] and Naoki Negishi[2]
[1] *Graduate School of Information Science and Technology, The University of Tokyo, Bunkyo-ku, Tokyo 113-8656, Japan*
[2] *Graduate School of Arts and Sciences, The University of Tokyo, Meguro-ku, Tokyo, 153-8902, Japan*
(Dated: April 15, 2022)

In this report, we simulate the time evolution of the $N = 3$ Heisenberg model by Tritterization on `ibmq_jakarta`, based on the circuit level approach (without pulse). Focusing on the symmetry of the Hamiltonian of the Heisenberg model, we construct and Trotterize an effective Hamiltonian on $(N - 1)$-qubit space which is encoded from the N particle Heisenberg model. We show this Trotterization of effective Hamiltonian is equivalent to changing the axis of the Trotterization of the original Hamiltonian. This encoding framework makes it possible to reduce the number of CNOT gates for one Trotter step from 6 to 4 in general, and when $N = 3$, the circuit depth and the number of CNOT gates becomes constant for any trotter steps. Combining with several error mitigation techniques, we finally achieve fidelity 0.98 ± 0.001 on `fake_jakarta` simulator, and 0.94 ± 0.001 on `ibmq_jakarta` real quantum device, for the given problem setting.

I. INTRODUCTION

The noisy two-qubit operation and the short coherent time are the two main factors that limits the ability of current near-term quantum computers. Previous researches imply even the depth 10 CNOT gate would destroy the genuine multipartite entanglement of GHZ state on IBM Quantum devices [1, 2]. This problem obviously arise in the given problem setting where we want to simulate the time evolution of Heisenberg model with multiple Trotter iterations.

In fact, the rigorous simulation of the Heisenberg model with Trotterzation would result in a deep quantum circuit. According to the sample program [3], one should use over 10 trotter iterations to achieve fidelity over 0.9 under noise-free simulation. In addition to this, Trotter iteration in this straightforward method requires at least depth $3 \times 2 = 6$ CNOT gates. When using the `fake_jakarta` noisy simulator, the fidelity could decreased into 0.1 with 12 Trotter iterations. Therefore, making the circuit shallower with less CNOT gates is the top priority to increase the fidelity under the current noise environment.

Towards this, some previous approaches adopt the quantum-classical hybrid algorithms [4, 5]. While they claim that the fidelity over 0.97 for the similar problem setting is achieved on IBM Quantum devices, their variational method requires heavy loops between quantum and classical process and requires many circuit implementations. In this sense, this might not be suitable under the limited shared quantum resources available within this Open Science Prize period.

Instead, we reduce the circuit depth and CNOT gates within the scope of ecosystem-friendly design. The idea is to focus on the unused symmetry in the given Hamiltonian, which allows us to embed the N sites Heisenberg model into $N - 1$-qubit system. Thanks to the commutativity of XXX Heisenberg Hamiltonian H_{Heis} with all the local Pauli-Z operators, all the eigenvectors of the Heisenberg Hamiltonian have even the degeneracy when the system size N is odd. The induces the relationship between the two degenerated orthogonal m-th eigenstates $|\phi_-^{(m)}\rangle$ and $|\phi_+^{(m)}\rangle$ as follows.

$$|\phi_-\rangle_i^{(m)} = \prod_{i=1}^{N} \sigma_z^i \, |\phi_+\rangle^{(m)} \tag{1}$$

This means the time evolution of the state initially given by linear combination of $\{\phi_-^{(m)}\}$ can be identified with that of $\{\phi_+^{(m)}\}$. Using this property, we succeed to embed the given N spin Heisenberg Hamiltonian into the equivalent effective Hamiltonian on $N - 1$ spin sites by an encoding unitary operator. The Trotterization on the effective Hamiltonian can be seen as taking a different axis of the Trotter decomposition. This would reduce the CNOT gates from 6 to 4 in one Trotter iteration for $N > 3$ case. When the system size is 3, the Trotter circuits only act on the two-qubit system with the same control-target qubits. In this case, a number of Trotter iterations can be fortunately optimized into constant depth circuit with constant number of CNOT gates, which greatly contributes to simulating the target state with surprisingly high fidelity.

Note that our proposed transformation scheme is "efficently" reduced from the theoretical inspection without any exponential computational cost to the system size N. In addition, the proposed method is "end-to-end" Trotterization algorithm which takes N-qubit initial state, simulates its time evolution with the modified Trotter axis in one circuit, and outputs the N-qubit target state. In this sense, we believe our method satisfies the requirements in the official rules: "Each submission must use Trotterization to evolve the specified state, under the specified Hamiltonian, for the specified duration with at least 4 Trotter steps." [6].

To obtain noiseless results, one may also apply the error mitigation techniques. Error mitigation techniques aims to recover the ideal expectation values via classical post-processing [7]. Here we use quantum readout error mitigation (QREM) and zero-noise exrapolation (ZNE).

The readout noise occurring in the measurement process is one of the significant noise on the current near-term devices. Since this noise can be characterized by an assignment stochastic matrix, we can perform its inverse on the noisy probability distribution. This is the base idea of the QREM method and we use the complete assignment matrix inversion prepared in the Qiskit-Ignis library [8].

We also applied ZNE [9] to the mitigated expectation values by QREM. The ZNE first tests the expectation values with different artificially scaled noise levels, and then extrapolate such noisy expectation values to estimate the "zero-noise" expectation. We used the unitary folding method [10] prepared in the Mitiq library [11]. Please install the mitiq package by 'pip install mitiq' before running the submitted programs. In addition, we also combined Pauli twirling [12] method with ZNE as applied in [4], where the improvement of the zero-noise expectation values is reported. Here we mitigated all the expectation values use for reconstruct the outcome density matrix. Since the quantum noise and mitigation noise may output the unphysical density matrix with negative eigenvalues, we found the closest positive semi-definite matrix by the maximum likelihood method [13].

As a result, we achieved the target state **fidelity over 0.99 on the noisy simulator** of `fake_jakarta`, and **over 0.94 on the real quantum device** of `ibmq_jakarta`. In the following experiments, we also checked the proposed method can simulate the time evolution from any initial states by both theoretical analysis and experiments. Therefore, we can say that the proposed method not only outputs high scores of the given problem setting of the contest, but also provides a practical solution for the simulation of Heisenberg model using Trotterization under more general situation.

The theoretical insight of the effective Hamiltonian of the Heisenberg model is mainly done by Naoki Negishi. The incorporation of the error mitigation and the code implementation is mainly done by Bo Yang. We solved the problem only by the circuit level optimization WITHOUT using Qiskit pulse.

II. THEORETICAL FOUNDATION

The XXX Heisenberg 3-spins Hamiltonian H_{Heis} is commutable with the products of σ_μ^i, ($\mu \in \{x, y, z\}$) for all sites as

$$[H_{\text{Heis}}, \sigma_\mu^1 \sigma_\mu^2 \sigma_\mu^3] = 0. \tag{2}$$

This Hamiltonian can be decomposed as a direct sum of the subspace

$$H_{\text{Heis}} \in \mathcal{H}_{\text{odd}} \oplus \mathcal{H}_{\text{even}}, \tag{3}$$

and $\mathcal{H}_{\text{odd,even}}$ is the the subspace composed by the eigenstates of $\sigma_z^1 \sigma_z^2 \sigma_z^3$ equal to $-1, 1$, that is

$$\mathcal{H}_{\text{odd}} = \{|100\rangle, |010\rangle, |001\rangle, |111\rangle\} \tag{4}$$

$$\mathcal{H}_{\text{even}} = \{|110\rangle, |101\rangle, |011\rangle, |000\rangle\}. \tag{5}$$

Any eigenvectors of H_{Heis} in the subspace $\mathcal{H}_{\text{odd}}$, defined as $|\text{odd}\rangle$ having the eigenenergy E, and the vector $\sigma_x^1 \sigma_x^2 \sigma_x^3 |\text{odd}\rangle \in \mathcal{H}_{\text{even}}$ is degenerated, so any states between $|\text{odd}\rangle \in \mathcal{H}_{\text{odd}}$ and $\sigma_x^1 \sigma_x^2 \sigma_x^3 |\text{odd}\rangle \in \mathcal{H}_{\text{even}}$ can be identified. In our strategy, we introduced effective Hamiltonian H_{eff} which gives the same time evolution for any initial state, reducing 2-spins state as $|ab\rangle_{\text{eff}}$ by identifying $|\text{odd}\rangle$ and $\sigma_x^1 \sigma_x^2 \sigma_x^3 |\text{odd}\rangle$ as

$$|000\rangle, |111\rangle \sim |00\rangle_{\text{eff}} \tag{6}$$

$$|011\rangle, |100\rangle \sim |01\rangle_{\text{eff}} \tag{7}$$

$$|110\rangle, |001\rangle \sim |10\rangle_{\text{eff}} \tag{8}$$

$$|101\rangle, |010\rangle \sim |11\rangle_{\text{eff}}, \tag{9}$$

where the symbol "$\sim$" represents equivalent relation. The time-dependent Schrödinger equation (TDSE) is governed by H_{eff} as

$$i\partial_t |\psi(t)\rangle_{\text{eff}} = H_{\text{eff}} |\psi(t)\rangle_{\text{eff}}, \tag{10}$$

and H_{eff} is constructed as

$$H_{\mathrm{eff}} = \sigma_x^1 + \sigma_x^2 + \sigma_z^1 + \sigma_z^2 - (\sigma_z^1\sigma_x^2 + \sigma_x^1\sigma_z^2), \tag{11}$$

consistently equal to the TDSE under the H_{Heis} in the 3-spins system. $\psi(t)$ is the wavefunction.

In addition, making the two kinds of projection operators $P_{+,-}$ to the subspace $\mathcal{H}_{\mathrm{even,odd}}$, respectively, we can rewrite H_{Heis} as

$$H_{\mathrm{Heis}} = \sum_{i\in\{+,-\}} P_i^\dagger H_{\mathrm{eff}}^{13} P_i, \tag{12}$$

where H_{eff}^{13} is given by Eq.(11) substituting $\boldsymbol{\sigma}^2 \to \boldsymbol{\sigma}^3$. Thus time propagation under the effective Hamiltonian is equivalent to that of the Hisenberg Hamiltonian, so we do not modified the specified Hamiltonian in this contest. The projection operator satisfies the following relations,

$$P_+ \in \mathcal{H}_{\mathrm{even}}, P_- \in \mathcal{H}_{\mathrm{odd}} \tag{13}$$

$$P_+P_-^\dagger = P_-P_+^\dagger = P_+^\dagger P_- = P_-^\dagger P_+ = 0 \tag{14}$$

$$P_+^\dagger P_+ = I_+ \in \mathcal{H}_{\mathrm{even}} \tag{15}$$

$$P_-^\dagger P_- = I_- \in \mathcal{H}_{\mathrm{odd}} \tag{16}$$

$$H_{\mathrm{eff}}^{13} \in \mathcal{H}_{\mathrm{odd}} \oplus \mathcal{H}_{\mathrm{even}}, \tag{17}$$

where $I_{+,-}$ is identity operator in the subspace $\mathcal{H}_{\mathrm{even,odd}}$, respectively. Because $P_+^\dagger H_{\mathrm{eff}}^{13} P_+$ and $P_-^\dagger H_{\mathrm{eff}}^{13} P_-$ are commutable, the time evolution operator $\exp(-iH_{\mathrm{Heis}}t)$ can be exactly separated into two parts,

$$\begin{aligned}
\exp(-iH_{\mathrm{Heis}}t) &= \exp(-iP_-^\dagger H_{\mathrm{eff}}^{13} P_- t)\exp(-iP_+^\dagger H_{\mathrm{eff}}^{13} P_+ t) && (18)\\
&= \{P_+^\dagger P_+ + P_-^\dagger \exp(-iH_{\mathrm{eff}}^{13} t) P_-\}\\
&\times \{P_-^\dagger P_- + P_+^\dagger \exp(-iH_{\mathrm{eff}}^{13} t) P_+)\}\\
&= \sum_{i\in\{+,-\}} P_i^\dagger \exp(-iH_{\mathrm{eff}}^{13} t) P_i. && (19)
\end{aligned}$$

Therefore, the time propagation is described by $\exp(-iH_{\mathrm{eff}}^{13}t)$. We Trotterize this time evolution operator into

$$\begin{aligned}
&\exp(-iH_{\mathrm{eff}}^{13}t)\\
&= \exp\left[-it\left\{(\sigma_x^1 + \sigma_z^2 - \sigma_x^1\sigma_z^2) + (\sigma_x^2 + \sigma_z^1 - \sigma_x^2\sigma_z^1)\right\}\right]\\
&= \lim_{n\to\infty}\left[e^{\frac{-it}{n}(\sigma_x^1+\sigma_z^2)} e^{\frac{it}{n}(\sigma_x^1\sigma_z^2+\sigma_x^2\sigma_z^1)} e^{\frac{-it}{n}(\sigma_x^2+\sigma_z^1)}\right]^n. \qquad (20)
\end{aligned}$$

Both of the first and third Trotter block can be given by local rotation-Z and rotation-X gates for each qubit. The second Trotter block is represented as 4×4 matrix given by

$$\begin{aligned}
&\exp\left[\frac{it}{n}(\sigma_x^1\sigma_z^2 + \sigma_z^1\sigma_x^2)\right]\\
&= \begin{pmatrix}
\cos^2\frac{t}{n} & i\sin\frac{t}{n}\cos\frac{t}{n} & i\sin\frac{t}{n}\cos\frac{t}{n} & \sin^2\frac{t}{n}\\
i\sin\frac{t}{n}\cos\frac{t}{n} & \cos^2\frac{t}{n} & -\sin^2\frac{t}{n} & -i\sin\frac{t}{n}\cos\frac{t}{n}\\
i\sin\frac{t}{n}\cos\frac{t}{n} & -\sin^2\frac{t}{n} & \cos^2\frac{t}{n} & -i\sin\frac{t}{n}\cos\frac{t}{n}\\
\sin^2\frac{t}{n} & -i\sin\frac{t}{n}\cos\frac{t}{n} & -i\sin\frac{t}{n}\cos\frac{t}{n} & \cos^2\frac{t}{n}
\end{pmatrix} \qquad (21)
\end{aligned}$$

This matrix is given by a 2-qubit circuit as the figure below (FIG.1).

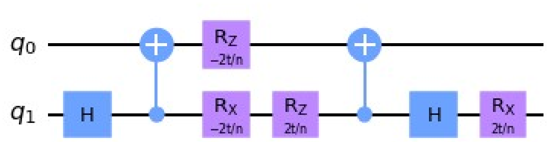

FIG. 1. The quantum gate of the second Trotter block given by Eq.(26)

Including with the first and third trotter blocks in Eq.(20) into the second, the unit of the Trotter step is represented as FIG.2.

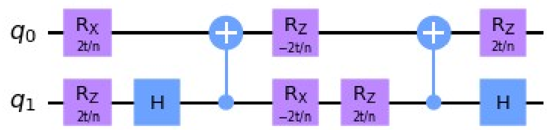

FIG. 2. The quantum gate of the Trotter unit given by Eq.(25)

The last task is the encoding and decoding of the initial and final state, respectively. In our method, we identify the 8 states in 3-spin states with the product between no time-evolving one particle state $|a\rangle_{\text{stat}}$ and time-evolving two-particle state $|bc\rangle_{\text{eff}}$under H^{23}_{eff} given by Eq.(17), as follows.

$$
\begin{aligned}
U_{\text{enc}}\,|000\rangle &= |000\rangle = |0\rangle_{\text{stat}}\,|00\rangle_{\text{eff}}\\
U_{\text{enc}}\,|011\rangle &= |001\rangle = |0\rangle_{\text{stat}}\,|01\rangle_{\text{eff}}\\
U_{\text{enc}}\,|110\rangle &= |010\rangle = |0\rangle_{\text{stat}}\,|10\rangle_{\text{eff}}\\
U_{\text{enc}}\,|101\rangle &= |011\rangle = |0\rangle_{\text{stat}}\,|11\rangle_{\text{eff}}\\
U_{\text{enc}}\,|111\rangle &= |100\rangle = |1\rangle_{\text{stat}}\,|00\rangle_{\text{eff}}\\
U_{\text{enc}}\,|100\rangle &= |101\rangle = |1\rangle_{\text{stat}}\,|01\rangle_{\text{eff}}\\
U_{\text{enc}}\,|001\rangle &= |110\rangle = |1\rangle_{\text{stat}}\,|10\rangle_{\text{eff}}\\
U_{\text{enc}}\,|010\rangle &= |111\rangle = |1\rangle_{\text{stat}}\,|11\rangle_{\text{eff}}
\end{aligned}
$$

where U_{enc} is the unitary operator to promote encoding, and the decoder of that is given by $U^{\dagger}_{\text{enc}}$. By the encoding and decoding, the circuit for the general solution of the time evolution under H_{Heis} can be represented as FIG.3

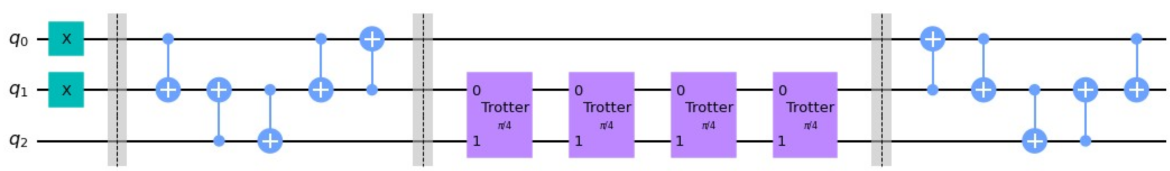

FIG. 3. The circuit gives the general solution of the time evolution by using Trotterization in this approach. Note that the number of Trotter steps on this figure is $n = 4$ case.

III. STRATEGIES: REDUCING CNOT GATE IN ENCODING AND DECODING

We made the general method of the time evolution governed by H_{Heis}. Ideally, the circuit in FIG.3 guarantees the exact time evolution in any initial state under $n \to \infty$. However, because the quantum gate of the encoding and decoding need to set 5 CNOT gates for each when we use ibm-jakarta, the noises are not perfectly removed for the high state tomography fidelity. In this section, we show the strategies to get much higher fidelity by reducing CNOT gates in encoding and decoding process by adapting the initial state conditions and time duration.

A. Considering initial condition

In this contest, the initial state is chosen as not entangled state, $|011\rangle$. This means that the encoding process never required CNOT gate in this method. Thus, it is only need to consider the decoding process. Analitically, the time propagation under H_{Heis} for the initial state of $|011\rangle$ is closed in the subspace $\mathcal{H}_{\text{even}}$. Thus we need to consider the decoding process as 4 states given by

$$\begin{aligned}
|000\rangle &= U_{\text{enc}}^{\dagger}|000\rangle \\
|011\rangle &= U_{\text{enc}}^{\dagger}|001\rangle \\
|110\rangle &= U_{\text{enc}}^{\dagger}|010\rangle \\
|101\rangle &= U_{\text{enc}}^{\dagger}|011\rangle .
\end{aligned}$$

This decoding process is given by 2 CNOT gates only, then the circuit in this strategy is given by FIG.5

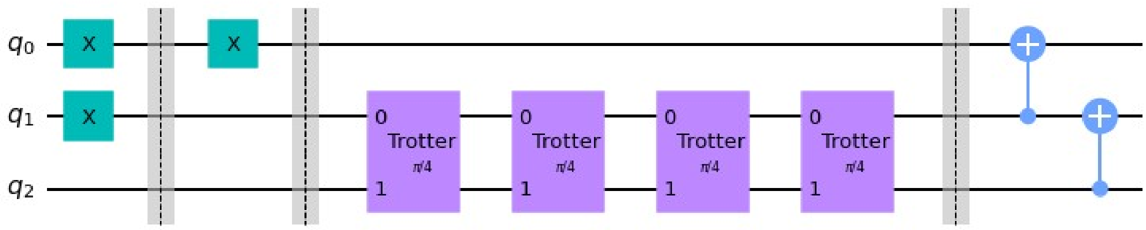

FIG. 4. The circuit giving the specific solution of the time evolution by using Trotterization of the H_{Heis} in this approach considering initial condition and subspace. Note that the number of Trotter steps on this figure is $n = 4$ case.

B. Considering time duration

If the Hamiltonian of the system is time independent, the time evolution is described by the eigenenergies E_i and vectors $|i\rangle$ as $|\psi(t)\rangle = \sum_i c_i e^{iE_i t}|i\rangle$. If the initial wavefunction is composed by more three eigenstates, the state vector $\psi(t)$ cannot return to the initial state $\psi(0)$. However, in the case of any gaps of the eigenenergies $\Delta_{ij} = E_i - E_j$ equal to the integer multiplication of a certain real value ϵ, that is $\Delta_{ij} \in \epsilon\mathbb{Z}$ for any i and j, the state completely return to the initial state in $t \in \frac{2\pi}{\epsilon}\mathbb{Z}$. In the case of H_{Heis}, we can proof $\Delta_{ij} \in 2\mathbb{Z}$ without diagonalization of 8×8 matrix. By introducing total Pauli matrix vector $\boldsymbol{\sigma}^{\text{tot}}$ defined as

$$\boldsymbol{\sigma}^{\text{tot}} = \boldsymbol{\sigma}^1 + \boldsymbol{\sigma}^2 + \boldsymbol{\sigma}^3, \tag{22}$$

the Hamiltonian is reconstructed as

$$\begin{aligned}
H_{\text{Heis}} &= \frac{1}{2}(\boldsymbol{\sigma}^{\text{tot}})^2 - \boldsymbol{\sigma}^1 \cdot \boldsymbol{\sigma}^3 - \frac{1}{2}\sum_i (\sigma^i)^2 \\
&= \frac{1}{2}(\boldsymbol{\sigma}^{\text{tot}})^2 - \boldsymbol{\sigma}^1 \cdot \boldsymbol{\sigma}^3 - \frac{9}{2} \\
&= \frac{1}{2}(\boldsymbol{\sigma}^{\text{tot}})^2 - \frac{1}{2}(\boldsymbol{\sigma}^1 + \boldsymbol{\sigma}^3)^2 - \frac{3}{2}
\end{aligned} \tag{23}$$

And we can show the commutation relation as

$$[H_{\text{Heis}}, \boldsymbol{\sigma}^{\text{tot}}] = 0. \tag{24}$$

Therefore, the eigenstate of this system also can be that of total spin square operator $(\boldsymbol{\sigma}^{\text{tot}})^2$. The eigenvalue of the operator can be written as,

$$\langle(\sigma^{\text{tot}})^2\rangle = S^{\text{tot}}(S^{\text{tot}} + 2) \tag{25}$$

where S^{tot} =3 or =1. The residual second term in Eq.(23) is also the summated spin square operator between $i = 1$ and $= 3$ site, and the eigenvalue is also known that it is given by Eq.(25) with $S^{\text{tot}} = 2$ or $= 0$. Then, substituting $(\boldsymbol{\sigma}^{\text{tot}})^2$ =15 or =3, and $(\boldsymbol{\sigma}^1 + \boldsymbol{\sigma}^3)^2$ =8 or =0, respectively, we can say $\Delta_{ij} \in 2\mathbb{Z}$ which guarantees that the state after the time duration $t = \pi$ in this system perfectly returns to initial state ($t = 0$) in any initial condition. It means that regarding the decoding process as inverse operation of encoding process is arrowed in $t \in \pi\mathbb{Z}$ case. In the case of the initial state equal to $|011\rangle$, the circuit can be represented by FIG.5. In such case, we can encode and decode without CNOT gate.

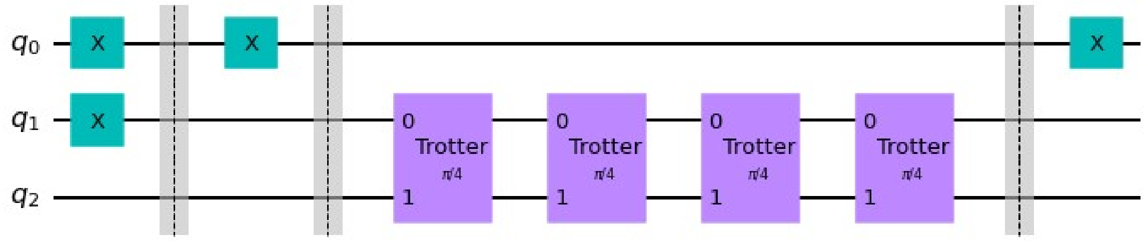

FIG. 5. The circuit giving the specific solution of the time evolution by using Trotterization of the H_{Heis} in this approach considering initial condition, subspace and time dulation $t \in \pi\mathbb{Z}$. Note that the number of Trotter steps on this figure is $n = 4$ case.

IV. ERROR MITIGATION

V. RUNNING ON SIMULATOR

The numerical simulation is conducted on both the `qasm_simulator` and the `fake_jakarta`.

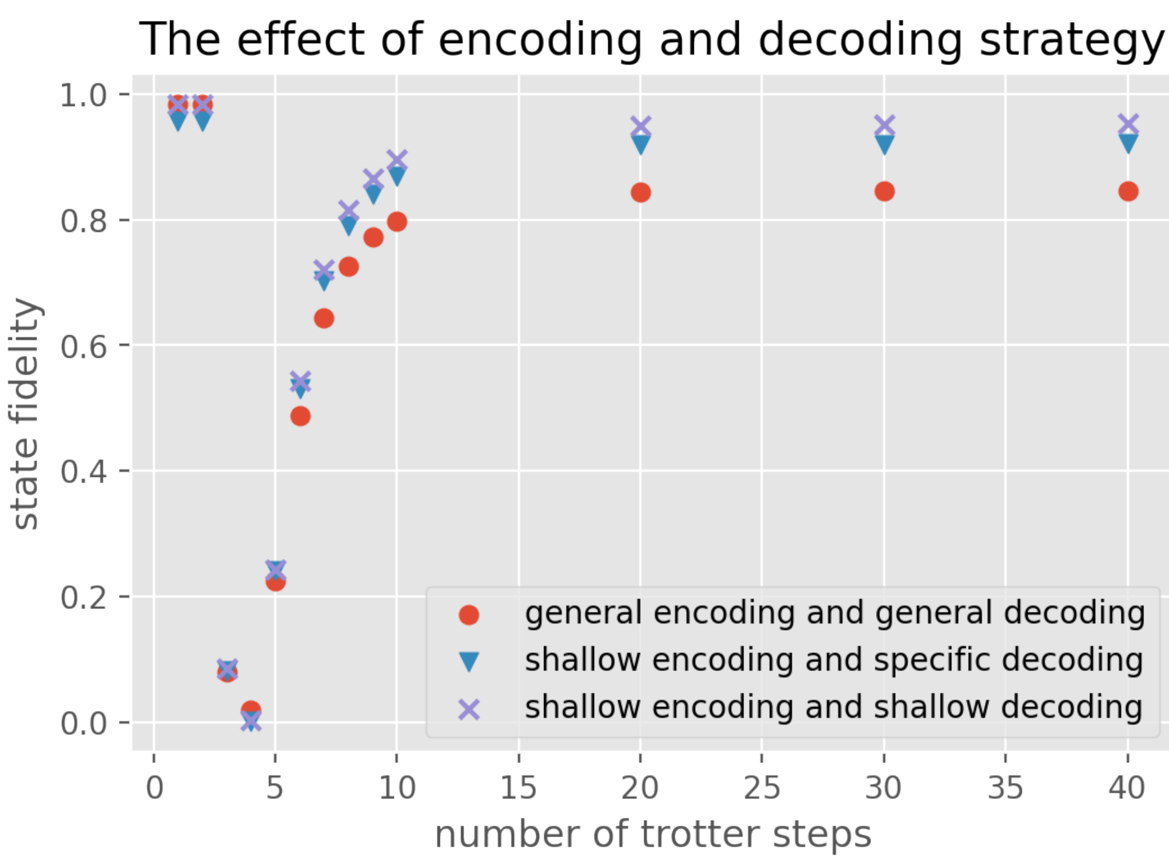

FIG. 6. Encoding strategy

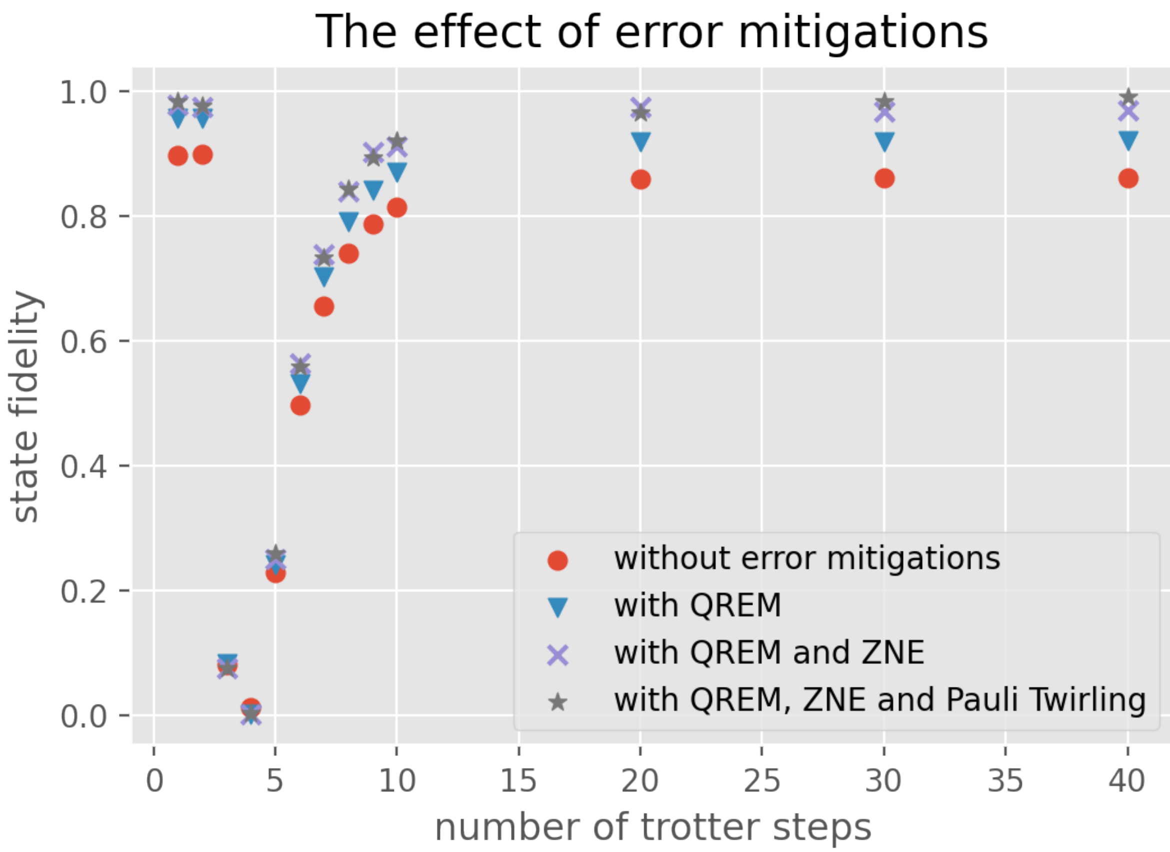

FIG. 7. Error mitigation

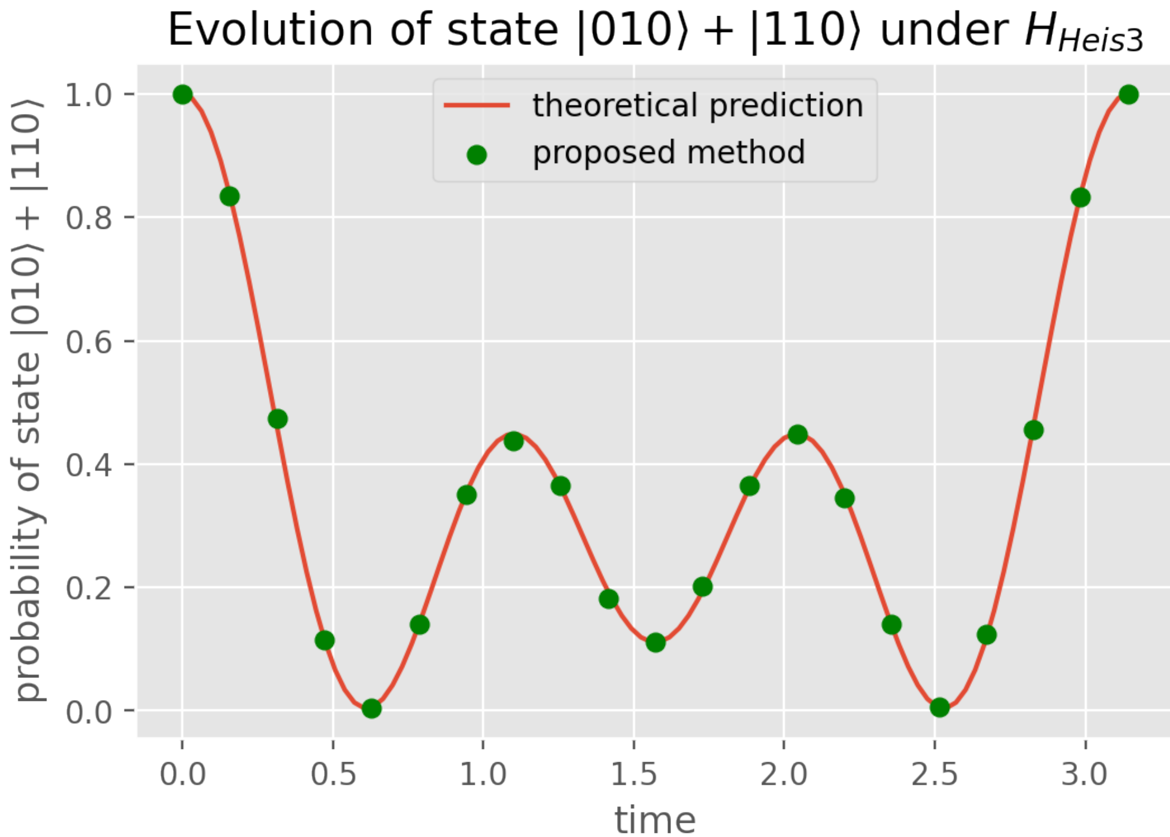

FIG. 8. Time evolution

VI. RUNNING ON REAL DEVICE

aaaaaaaaaaaaaaaaaaaaaaaaa

VII. CONCLUSION

future work
- increase shot count for zne - combine other error mitigation

ACKNOWLEDGMENTS

To AJ and other staffs.

[1] B. Yang, R. Raymond, and S. Uno, An efficient quantum readout error mitigation for sparse measurement outcomes of near-term quantum devices (2022).
[2] G. J. Mooney, G. A. L. White, C. D. Hill, and L. C. L. Hollenberg, Journal of Physics Communications **5**, 095004 (2021).
[3] IBM Quantum Awards: Open Science Prize 2021, `https://github.com/qiskit-community/open-science-prize-2021`.
[4] N. F. Berthusen, T. V. Trevisan, T. Iadecola, and P. P. Orth, Quantum dynamics simulations beyond the coherence time on nisq hardware by variational trotter compression (2021).
[5] C. Cîrstoiu, Z. Holmes, J. Iosue, L. Cincio, P. J. Coles, and A. Sornborger, npj Quantum Information **6**, 10.1038/s41534-020-00302-0 (2020).

[6] Official Rules of IBM Quantum Awards: Open Science Prize 2021, https://res.cloudinary.com/ideation/image/upload/w_870/jug8tjgy6egm26zojyxd.pdf.

[7] S. Endo, Z. Cai, S. C. Benjamin, and X. Yuan, Journal of the Physical Society of Japan **90**, 032001 (2021).

[8] G. Aleksandrowicz, T. Alexander, P. Barkoutsos, L. Bello, Y. Ben-Haim, D. Bucher, F. J. Cabrera-Hernández, J. Carballo-Franquis, A. Chen, C.-F. Chen, J. M. Chow, A. D. Córcoles-Gonzales, A. J. Cross, A. Cross, J. Cruz-Benito, C. Culver, S. D. L. P. González, E. D. L. Torre, D. Ding, E. Dumitrescu, I. Duran, P. Eendebak, M. Everitt, I. F. Sertage, A. Frisch, A. Fuhrer, J. Gambetta, B. G. Gago, J. Gomez-Mosquera, D. Greenberg, I. Hamamura, V. Havlicek, J. Hellmers, Łukasz Herok, H. Horii, S. Hu, T. Imamichi, T. Itoko, A. Javadi-Abhari, N. Kanazawa, A. Karazeev, K. Krsulich, P. Liu, Y. Luh, Y. Maeng, M. Marques, F. J. Martín-Fernández, D. T. McClure, D. McKay, S. Meesala, A. Mezzacapo, N. Moll, D. M. Rodríguez, G. Nannicini, P. Nation, P. Ollitrault, L. J. O'Riordan, H. Paik, J. Pérez, A. Phan, M. Pistoia, V. Prutyanov, M. Reuter, J. Rice, A. R. Davila, R. H. P. Rudy, M. Ryu, N. Sathaye, C. Schnabel, E. Schoute, K. Setia, Y. Shi, A. Silva, Y. Siraichi, S. Sivarajah, J. A. Smolin, M. Soeken, H. Takahashi, I. Tavernelli, C. Taylor, P. Taylour, K. Trabing, M. Treinish, W. Turner, D. Vogt-Lee, C. Vuillot, J. A. Wildstrom, J. Wilson, E. Winston, C. Wood, S. Wood, S. Wörner, I. Y. Akhalwaya, and C. Zoufal, Qiskit: An Open-source Framework for Quantum Computing (2019).

[9] K. Temme, S. Bravyi, and J. M. Gambetta, Phys. Rev. Lett. **119**, 180509 (2017).

[10] T. Giurgica-Tiron, Y. Hindy, R. LaRose, A. Mari, and W. J. Zeng, in *2020 IEEE International Conference on Quantum Computing and Engineering (QCE)* (IEEE, 2020).

[11] R. LaRose, A. Mari, N. Shammah, P. Karalekas, and W. Zeng, Mitiq: A software package for error mitigation on near-term quantum computers, https://github.com/unitaryfund/mitiq (2020).

[12] Y. Li and S. C. Benjamin, Phys. Rev. X **7**, 021050 (2017).

[13] J. A. Smolin, J. M. Gambetta, and G. Smith, Phys. Rev. Lett. **108**, 070502 (2012).

Appendix A: Soruce Code

aaaaaaaaaaaaaaaaaaaaaaaaa